Comparative Study of Density Profiles in Two Divertor Plasma Simulators : DiPS and MP^2

H.-J. Woo[1], K.-S. Chung[1], H.-J. You[1], T. Lho[2], Y.H. Jung[2], K.-K Choh[2], J.-S. Yoon[2], B. Lee[2], S.-J. Yoo[2], and M. Kwon[2]

[1]*Div. of Electrical &Biomedical Eng, Hanyang University, Seoul 133-791, Korea*
[2] *National Fusion Research Center, Daejeon 305-333, Korea*

Recently, the MP^2 (Multi-Purposed Plasma) facility has been developed with the honeycomb-like large area LaB_6 cathode with 8 inches diameter. One LaB_6 plate has been arranged in the cathode centre with 4 inch diameter and six LaB_6 plates are located at the outer region with 2 inch diameter. These LaB_6 plates are heated by graphite heater separately. Density profile (or ion saturation current profile) of MP^2 is different from that of DiPS (Diversified Plasma Simulator), which is also based upon the LaB_6 cathode but it has only one LaB_6 plate with 4 inch diameter. Comparing with DiPS, the outer cathodes of MP^2 control the density profile between the core plasma (or ionization region) and the edge plasma (or recombination region), and difference is more clearly appeared during the high magnetic field operation. Density profiles of MP^2 and DiPS are presented for two cases: magnetic field strengths of 435 and 870 G.

1. Introduction

Hanbit mirror device[1] has been renovated as a Multi-Purpose Plasma (MP^2) facility for the divertor plasma simulation, space propulsion, and astrophysical research. During the first renovation stage, the divertor plasma simulator had been developed with the LaB_6 cathode. Since the LaB_6 has a high thermal electron emission rate, low evaporation rate and high resistance on contamination in case of vacuum break, the LaB_6 cathode has been used for plasma generation in most divertor plasma simulators such as PISCES A[2] & B[3], PSI-II[4], NAGDIS-II[5], TPD-sheetIV[6], MAP-II[7], and DiPS[8]. However, the LaB_6 plate can be easily broken from its weakness against the thermal shock. Hence, it is hard to make the large area LaB_6 cathode over 15 cm in diameter with one LaB_6 plate.

The thermal stresses on the LaB_6 are originated by non-uniformity and sudden temporal variation of the temperature on the LaB_6 surface. The former might be caused by the non-uniform heating of LaB_6 cathode by the external heaters and by concentration of heat fluxes by plasma, especially ions, on small portions of LaB_6 surface. These are hard to resolve because the heat and the heat fluxes of cylindrical plasma are naturally concentrated on the centre position geometrically although one efforts to spread the heat on the LaB_6 surface by larger heaters than LaB_6 size or to make the null point with cusp magnetic field. The latter one takes place when rapid heating of LaB_6 and the current overflow in a flash on the LaB_6 surface. This can solved if one increases the heater power slowly and uses the discharge power supply with good feed back control. Honeycomb-like large area LaB_6 (HLA-LaB_6) cathode is composed of the multiple array of LaB_6 plate with small diameter, for increasing the life time of LaB_6 by reducing the thermal stress. The concept of HLA-LaB_6 cathode is based upon increasing thermal resistance on the non-uniform heating problems with multiple array of small LaB_6 plate.

In this work, the initial plasma density profiles of HLA-LaB_6 (MP^2) and one LaB_6 cathode (DiPS)[8] are compared with Ar plasma in the two magnetic field profiles.

2. Design Concept of MP^2

Figure 1 shows the schematic diagram of the MP^2 and its magnetic profiles. The MP^2 is composed of

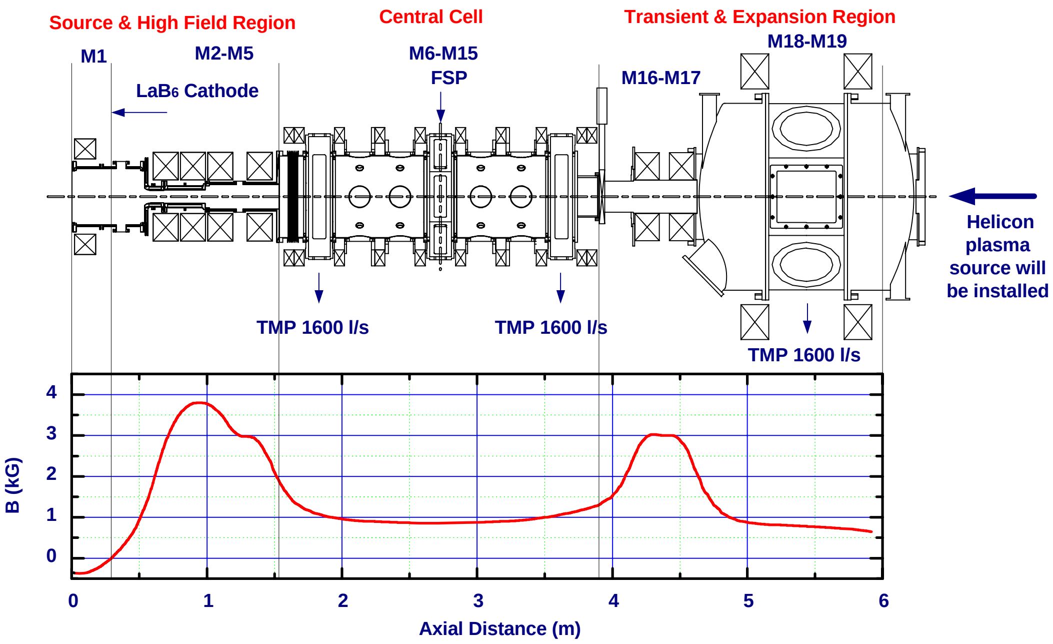

Fig. 1: Schematic diagram of MP^2 and its magnetic field profile (MF2 field configuration).

source and high field region, central cell, transient and expansion region with 19 electromagnets.

The source region of MP^2 is composed of source chamber, floating electrode, anode and high field chamber. In this region, all components have the double wall configuration for preventing the vacuum break from the high heating powers of LaB_6 cathode and high density plasma. The dimensions of the source chamber, floating electrode, anode and high field chamber are 412 mm (I.D.: inner diameter) x 520 mm (L: length), 90 mm (I.D.) x 140 mm (L), 100 mm (I.D.) x 300 mm (L), and 180 mm (I.D.) x 550 mm (L), respectively. Teflon insulators with the thickness of 10 mm are located between source flange and source chamber, source chamber and floating electrode, and floating electrode and anode for its electrical insulation. The HLA-LaB_6 cathode surface is located at the null point (or minimum B) with cusp magnetic field configuration for producing the high density plasma by focusing the electrons and for reducing the thermal stresses on LaB_6 surface from ion bombardment heating by diverging the ions with magnetic field lines simultaneously.

Figure 2 shows the arrangement of LaB_6 plates, which is composed of one inner LaB_6 cathode with 4 inch of diameter and six outer LaB_6 cathodes with 2 inch of diameter. The LaB_6 cathode arrays are separately heated by inner and outer graphite heaters.

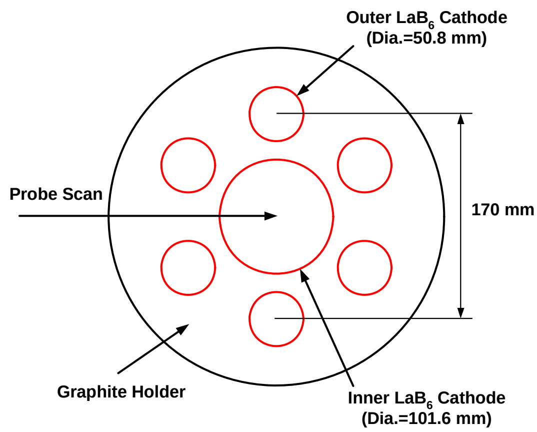

Fig. 2: Arrangement of LaB_6 plates in HLA-LaB_6 Cathode

The first plasma is generated with Ar gas in the following conditions: (1) Two magnetic field conditions of MF1 [-150 A (M1), 200 A (M2-M5, M16-M19), 350 A (M6-M15)] and MF2 [-300 A (M1), 400 A (M2-M5, M16-M19), 700 A (M6-M15)], (2) Neutral pressures of 30 mTorr (at source chamber) and 2.5 mTorr (at central cell), (3) Discharge voltage of 60 - 65 V, discharge currents of 5 - 45 A, and (5) LaB6 heating powers of 3.69 kW (250 A -14.74 V) for inner heater and 14.79 kW (390 - 37.9 V) for outer heater. The radial profiles of plasma density and electron temperature are measured by single probe with 0.5 mm (diameter) and 4 mm (length), which installed on the fast scanning probe (FSP) system at the middle of central cell.

3. Experiment and Data

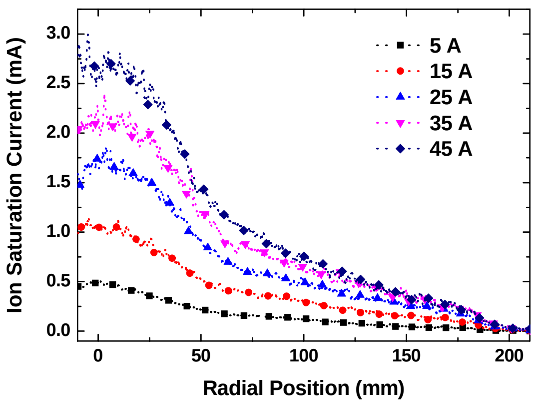

(a)

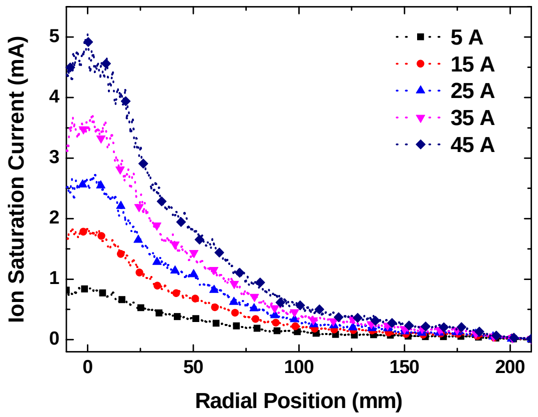

(b)

Fig. 3: Ion saturation current profiles (a) MF1 field configuration, and (b) MF2 Field Configuration

Figure 3 shows the radial distributions of ion saturation currents with the discharge currents from 5 A to 45 A at two magnetic field configurations of MF1 and MF2 cases. The magnetic field intensities are 435 G and 870 G at measurement position (FSP in Fig. 1) in the two magnetic field configurations of MF1 and MF2, respectively. The half- and e-folding lengths, which represent the plasma column size, are 52 mm (MF1) and 35 mm (MF2), and 78 mm (MF1) and 55 mm (MF2), respectively. Normalized ion saturation currents of MP2 and DiPS are shown in Fig. 4. The ion saturation currents are normalized by the ion saturation currents at plasma center, I_0, and the radial position is also normalized by the plasma size, $r/r(I/I_0=0.03)$, which is defined as the plasma edge for our convenience.

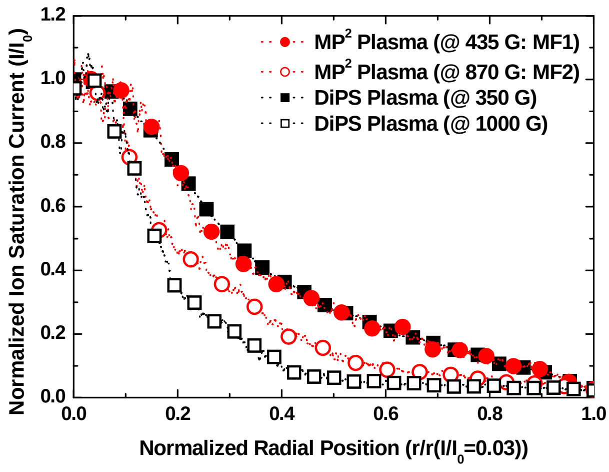

Fig. 4: Normalized Ion Saturation Current Profile

In the low field regime (< 500 G), there is almost no difference in radial ion saturation currents between HLA-LaB_6 of MP^2 and one of DiPS. In the high field regime (~ 1000 G), however, the profile of ion saturation current of HLA-LaB_6 has been observed milder than that of DiPS for $r/r(I/I_0=0.03) = 0.12$ (or 22 mm of the radial position). Although plasma generation with only the inner cathode of MP^2 is not done in this experiment, one can expect that it has almost same profiles of ion saturation currents in MP^2 and DiPS, because their size and property are almost the same. This might be caused by spatial localizations of the outer LaB_6 cathode contributions by decreasing the cross-field diffusion with magnetic field intensity although they have same magnetic flux profile in the HLA-LaB_6 of MP^2. Radial density profiles and electron temperatures measured by single probe are shown in Fig. 5 at MF2 field configuration. Plasma densities and electron temperature are 2.6 x 10^{12} cm^{-3} and 3.4 eV, respectively. The plasma densities are monotonically decreased with radial position, but the electron temperatures seem to be almost constants within the radius of 15 mm in MF2 field configuration. It is also expected the outer cathode contributions from the flat profiles of electron temperatures.

4. Summary

Multi-Purpose Plasma (MP^2) facility, as a renovated Hanbit device, is composed of the divertor plasma, astrophysics, and space propulsion simulators, among which the divertor plasma simulator had been developed with honeycomb-like large area LaB_6 (HLA-LaB_6) cathode and its initial plasma characteristics are measured by a fast-scanning single probe.

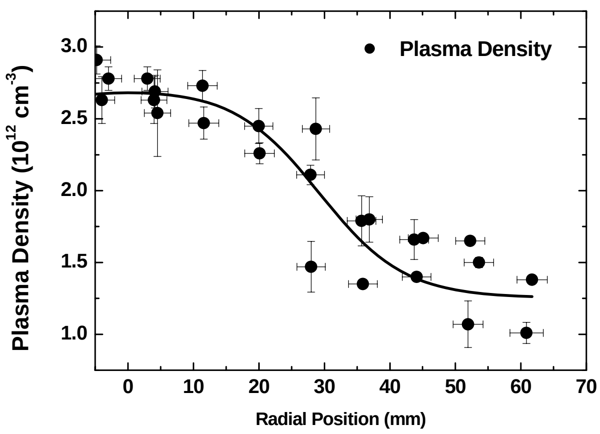

(a)

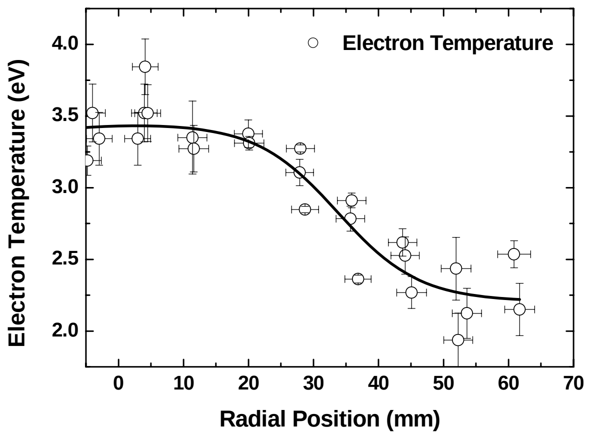

(b)

Fig. 5: Plasma density and electron temperature profile at MF2 field configuration in MP^2 (a) plasma density, and (b) electron temperature.

The HLA-LaB_6 cathode can be easily generated the high density plasma and large area over 20 cm in diameter, which depends on magnetic field configuration, by overcoming the problems of its weakness against the thermal shock. In the high magnetic field configuration, it is clearly shown the outer LaB_6 cathode contribute on the plasma density from radial profiles of the ion saturation currents in Figs. 3 and 4 by shrinking the cross-field diffusion. Although contribution from the outer cathodes are not clearly observed in low field regime like it in high field regime, one can expect that it is mixed up the inner and outer contributions from the flat profiles of the electron temperatures, which is not decreased monotonically. The measured plasma densities is reached up to 2.6×10^{12} cm^{-3} and the electron temperature is 3.4 eV at 45 A of discharge currents and MF2 field configuration. In the near future, the optimization of HLA-LaB_6 plasmas will be preceded with the different heater powers for inner and outer LaB_6 cathodes, discharge powers up to 100 A, magnetic field configurations, and the gas species of Ar, He, and H_2 for the radial profiles of plasma densities and electron temperatures and its magnitudes.

5. References

[1] M. Kwon et al., Nucl. Fusion **47**, 17 (2005).
[2] D. M. Goebel, J. T. Crow, and A. T. Forrester, Rev. Sci. Intrum. **49**, 469 (1978).
[3] Y. Hirooka et al., J. Vac. Sci. Technol. A **8**, 1790 (1990).
[4] B. Koch, Ph.D dissertation, Humboldt University, Berlin (2004).
[5] N. Ohno et al., Nucl. Fusion **41**, 1055 (2001).
[6] M. Ono, A. Tonegawa, K. Kumita, T. Shibuya, and K. Kawamura, J. Nucl. Mater. **337-339**, 261 (2005).
[7] S. Kado, H. Kobayashi, T. Oishi, and S. Tanaka, J. Nucl. Mater. **313-316**, 754 (2003).
[8] K.-S. Chung, H.-J. Woo, G.-S. Choi, J.-J. Do, Y.-J. Seo, and H.-J. You, Contrib. Plasma Phys. **46**, 354 (2006).